PKMζ-PKCι/λ double-knockout demonstrates atypical PKC is crucial for the persistence of hippocampal LTP and spatial memory

Authors:
Panayiotis Tsokas[1,2,3], Changchi Hsieh[1], Alejandro Grau-Perales[4], Andrew Tcherepanov[1], Leo Kwok[4], Laura Melissa Rodriguez-Valencia[1,2], David A. Cano[5], Kim D. Allen[1,3,6], Hannah J. H. Smith[1,7], Sabina Kubayeva[5], Benson J. Wei[1], Samuel Sabzanov[5], Rafael E. Flores-Obando[1], Sourav Ghosh[8], Peter John Bergold[1,9], Jerry Rudy[10], James E. Cottrell[2], André Antonio Fenton[1,4,11]*, Todd Charlton Sacktor[1,2,9]*

Affiliations:

[1]Department of Physiology and Pharmacology, The Robert F. Furchgott Center for Neural and Behavioral Science, State University of New York Downstate Health Sciences University; Brooklyn, New York 11203, USA.

[2]Department of Anesthesiology, State University of New York Downstate Health Sciences University; Brooklyn, New York 11203, USA.

[3]Department of Pathology, State University of New York Downstate Health Sciences University; Brooklyn, New York 11203, USA.

[4]Center for Neural Science, New York University; New York, New York 10003, USA.

[5]College of Medicine, State University of New York Downstate Health Sciences University; Brooklyn, New York 11203, USA

[6]Department of Biology, City University of New York-Medgar Evers College; Brooklyn, New York 11225, USA

[7]Currently, Department of Neuroscience and Cell Biology, Rutgers University; New Brunswick, New Jersey 08901, USA.

[8]Departments of Neurology and Pharmacology, Yale University; New Haven, Connecticut 06520, USA

[9]Department of Neurology, State University of New York Downstate Health Sciences University; Brooklyn, New York 11203, USA.

[10]Department of Psychology and Neuroscience, University of Colorado at Boulder; Boulder, Colorado 80302, USA.

[11]Neuroscience Institute at NYU Langone Medical Center; New York, New York 10016, USA.

*Corresponding authors. Emails: tsacktor@downstate.edu, afenton@nyu.edu

Abstract:

Is long-term memory maintained by stable synaptic structures or persistent biochemical action? PKMζ, a persistently active atypical PKC (aPKC), is thought to be crucial for maintaining the late phase of long-term potentiation (late-LTP) and long-term memory through sustained kinase action. However, PKMζ-knockout mice express hippocampal LTP and spatial memory while lacking neocortical LTP, calling into question whether persistent kinases and PKMζ are fundamental to LTP and memory. In Tsokas et al., 2016, we showed PKCι/λ, the other aPKC, becomes persistently active in PKMζ-knockout mice. In wild-type mice, PKCι/λ is critical to the initial generation of early-LTP and short-term memory, and PKMζ compensates for genetic deletion of PKCι/λ by supporting both early- and late-phase processes. Here, we tested whether PKCι/λ compensates for the loss of PKMζ by genetically ablating both aPKCs. Whereas deleting PKMζ and PKCι/λ individually induces compensation, deleting both aPKCs abolishes hippocampal late-LTP. Hippocampal ι/ζ-double-knockout eliminates spatial long-term memory but not short-term memory. Thus, in the absence of PKMζ, a second persistent biochemical process compensates to maintain late-LTP and long-term memory.

Introduction

The prevailing textbook mechanism for how memory is retained asserts that stable structural changes at synapses, the result of initial protein synthesis and growth, sustain memory without the need for ongoing biochemical activity dedicated to storing information. This idea, as introduced, hypothesized, and established by Ramón y Cajal, Hebb, and Kandel, has led to identifying structural plasticity, and structural components of synapses that contribute to establishing LTP and memory (*Ramón y Cajal, 1894; Hebb, 1949; Bailey and Kandel, 1993*), including cytoskeletal actin and perineuronal nets (*Matus, 2000; Tsien, 2013*). In contrast to non-enzymatic, stable changes in structure, memory could also be sustained by ongoing, persistent biochemical processes, a key alternative hypothesis independently proposed by Crick, Lisman, and Schwartz (*Crick, 1984; Lisman, 1985; Schwartz, 1993*).

The search for biochemical processes that maintain long-term potentiation (LTP) for hours and long-term memory for days has focused on the persistently active protein kinases, CaMKII and PKMζ. The kinase action of CaMKII is only crucial for initiating but not perpetuating LTP and memory (*Sacktor and Fenton, 2018; Tullis et al., 2023; Bayer and Giese, 2024*). In contrast, under normal circumstances, the autonomously active, atypical PKC (aPKC) isoform PKMζ is thought to play a critical role in maintaining the enduring late phase of LTP and long-term memory (*Pastalkova et al., 2006; Shema et al., 2007; Shema et al., 2011; Wang et al., 2016; Tsokas et al., 2024*). Application of zeta-inhibitory peptide (ZIP) that suppresses both PKMζ and PKCι/λ, a closely related aPKC, reverses late-LTP, even after a day (*Pastalkova et al., 2006; Madronal et al., 2010*). (Hereafter PKCι/λ is referred to as PKCι.) ZIP also erases enduring long-term memory for specific but not general types of information, days (*Serrano et al., 2008; Gao et al., 2018*) and even months (*Pastalkova et al., 2006; Shema et al., 2007*) after memory acquisition without impairing new learning. There is concern that the inhibitory effects of ZIP on LTP and memory maintenance may not be due to its targeting PKMζ or PKCι, but to its off-target effects (*Sadeh et al., 2015; LeBlancq et al., 2016; Stokes et al., 2025*). Nonetheless, multiple second-generation PKMζ-specific inhibitors, PKMζ-antisense oligodeoxynucleotides, and PKMζ-shRNA also disrupt late-LTP and long-term memory (*Tsokas et al., 2016; Wang et al., 2016; Tsokas et al., 2024*).

If PKMζ is genetically deleted, however, the key long-term processes of hippocampal LTP and long-term memory appear normal and are still inhibited by ZIP (*Lee et al., 2013; Volk et al., 2013; Tsokas et al., 2016*). In contast, in the same mutant mice LTP is eliminated in medial prefrontal cortex (mPFC) (*Kniffin et al., 2025; Sacktor, 2025*). These results appear contradictory, suggesting that PKMζ alone may be essential for LTP maintenance in mPFC, whereas either other ZIP-sensitive molecules compensate for PKMζ in the hippocampus, or an enduring structural change sustains LTP and memory in the absence of *Prkcz*, the PKMζ gene. In Tsokas et al., 2016, several members of the PKC gene family were found to increase expression in compensation for the loss of PKMζ, and PKCι was the most promising candidate, as closely related genes often functionally compensate (*Gu et al., 2003; Conant and Wagner, 2004; White et al., 2013; El-Brolosy and Stainier, 2017*). Notably, PKCι is critical to the initial generation of the early phase of LTP and short-term memory (*Ren et al., 2013; Tsokas et al., 2016; Wang et al., 2016; Sheng et al., 2017*), and PKMζ compensates for its genetic deletion, supporting both short- and long-term processes (*Sheng et al., 2017*). Perhaps instead of a structural change from activity-dependent growth, LTP and long-term memory maintenance might require a persistent kinase after all — but not always PKMζ.

The notion that persistent PKCι is a biochemical mechanism responsible for late-phase LTP and long-term memory when PKMζ is genetically deleted raises two questions: 1) Does PKCι persist in LTP and long-term memory in the absence of PKMζ, and 2) Does eliminating the two biochemical mechanisms abolish enduring LTP and long-term memory? We address these questions using conditional and double-knockout strategies.

Results

As neither inducible nor constitutive PKMζ gene ablation eliminates hippocampal LTP (*Volk et al., 2013*), it is important to know if compensatory increases in other PKCs are present in the hippocampus of conditional PKMζ-KO mice (ζ-cKO), as observed in PKMζ-null mice (*Tsokas et al., 2016*). In PKMζ-null mouse hippocampus, basal levels of PKCι and the conventional PKCβI specifically increased (*Tsokas et al., 2016*). To examine ζ-cKO mouse hippocampus, adult CaMKIIα promoter-driven-CreER^{T2}Prkcz$^{fl/fl}$ mice were injected with tamoxifen. One week later, expression of PKMζ in hippocampus decreased, and there was a compensatory increase in PKCι, as well as PKCι phosphorylated on its activation-loop (Figure 1A, Figure 1 — figure supplement 1A, Figure 1 — table supplement 1A, 2A). In addition, the expression of all four conventional PKCs (α, βI, βII, γ) increased, as did phosphorylation of the conventional PKC activation-loop (Figure 1B, Figure 1 — figure supplement 1A, table supplement 1B, 2A). However, there was no change in the expression of the four novel PKC isoforms (δ, ε, η, θ) or phosphorylation of the activation-loop of PKCε (Figure 1B, Figure 1 — figure supplement 1A, table supplement 1B, 2A). There also was no change in either the level of CaMKIIα, which is critical for LTP induction (*Bayer and Giese, 2024*), or T286-autophosphorylation of CaMKIIα, which induces Ca^{2+}-independent autonomous kinase activity (*Miller and Kennedy, 1986*) (Figure 1 — figure supplement 1B, table supplement 2B). Thus, conditional and constitutive PKMζ-KO mice express similar compensatory increases in PKCι, as well as other PKCs, in hippocampus.

Does the increase in PKCι persist in long-term memory, such that one biochemical process substitutes for the other? Previous research has shown that PKMζ expression in CA1 *stratum (st.) radiatum* of wild-type (WT) mice remains elevated for at least a month after training on a spatial memory task (*Hsieh et al., 2021; Han et al., 2025*). We determined if PKMζ-cKO mice would also exhibit a compensatory increase of PKCι in *st. radiatum*. PKMζ was ablated in CaMKIIα-promoter-driven-CreER^{T2}Prkcz$^{fl/fl}$ mice. Three weeks later, they were trained on the active place avoidance task (Figure 1C, Figure 1 — figure supplement 2). One week after training, compared to vehicle-injected littermates, the PKMζ-cKO showed a decrease to ~25% in PKMζ expression and an increase to ~400% in PKCι expression (Figure 1C, Figure 1 — table supplement 1C). Thus, ζ-cKO induces compensatory persistently increased expression of PKCι.

Does the persistent PKCι mechanism functionally substitute for that of PKMζ in LTP and long-term memory of PKMζ-KO mice? As PKCι-null mice are embryonically lethal (*Seidl et al., 2013*), we determined the functional significance of the compensatory increase of PKCι for LTP by injecting an adeno-associated virus (AAV) expressing Cre-recombinase in one hippocampus of PKCι-floxed/PKMζ-null mice (*Prkci$^{fl/fl}$-Prkcz$^{-/-}$*) mice (*Sheng et al., 2017*) (Figure 2). The contralateral hippocampus was injected with a control AAV-eGFP, and *ex vivo* slices prepared for electrophysiology. PKCι decreased in the ipsilateral hippocampus to ~20%

compared to the contralateral hippocampus (Figure 2). If PKC ι is important for enduring LTP in PKM ζ-KO mice, then this decrease should disrupt LTP. High-frequency stimulation (HFS) of the Schaffer collateral/commissural-CA1 synapses in the ipsilateral ι/ζ-dKO slices produced no persistent change in the residual PKC ι and a transient LTP only lasting ~1-2 h (Figures 2, 3A). In contrast, HFS of the contralateral slices with PKC ι but lacking PKM ζ induced persistent increases of the PKC ι to ~200% and late-LTP, both lasting at least 3 h, the duration of the recordings (Figures 2 and 3A). In addition, slices from hippocampus of PKC ι-floxed/PKM ζ-null mice injected with AAV expressing Cre by the CaMKIIα-promoter to selectively delete PKC ι in excitatory neurons resulted in similar transient LTP (Figure 3A, inset; Figure 3 — figure supplement 1A). The virus injected into PKC ι-floxed mice that express PKM ζ (*Prkci*$^{fl/fl}$-*Prkc*$^{+/+}$ mice) resulted in compensated LTP as in previous reports (*Sheng et al., 2017*) (Figure 3 — figure supplement 1B). Thus, deleting the aPKCs individually produces compensation, whereas deleting both aPKCs eliminates late-LTP.

We tested if late-LTP could be induced in ι/ζ-dKO hippocampus by increasing HFS from two trains, 20 sec apart, which is optimized to produce an early onset of late-LTP (*Tsokas et al., 2007*), to four trains, spaced 5 min apart, which is optimized to produce maximal late-LTP (*Scharf et al., 2002; Serrano et al., 2005*) (Figure 3B). Stronger stimulation induces LTP in ι/ζ-dKO slices that lasts only ~1-2 h. This LTP was no longer expressed at 3 h post-stimulation, at which time field excitatory postsynaptic potentials (fEPSPs) did not significantly differ from baseline fEPSPs before HFS.

To determine if PKC ι supports long-term memory in the absence of PKM ζ, we trained mice on the active place avoidance task (Figure 4A). We compared the effects of double-knockout (ι/ζ-dKO) to single knockout (ζ-KO), by injecting *PKC ι*$^{fl/fl}$-*PKM ζ*$^{-/-}$ littermates bilaterally in hippocampus with either AAV-Cre or AAV-eGFP. Mice received 3, 30-min training trials separated by 24 hours and a final retention test without shock the next day. Our measure of short-term memory was maximum avoidance time within each session (Figure 4B). Maximum avoidance time reflects the time between shocks, which is controlled by the animal's behavior and within-trial memory. Note that compared to pretraining inter-shock zone entries, the maximum avoidance time for ζ-KOs and ι/ζ-dKOs greatly increased. This indicates that they both had short-term memory for the shock zone. Our measure of long-term memory was time to first entry into the shock zone at the beginning of each session (Figure 4C). This reflects their long-term memory maintained across days from previous trials. ζ-KOs first entry times increased dramatically from pretraining to both session 3 and retention test, indicating that mice with PKC ι maintain long-term memory. In contrast, ι/ζ-dKO mice displayed a minimal increase at session 3 that was not significantly different from pretraining, and no detectable difference between pretraining and the retention test, indicating minimal or no spatial long-term memory.

Discussion

Although the structural model of memory storage is the standard account (*Bailey and Kandel, 1993*), the maintenance of hippocampal LTP and long-term memory in WT mice appeared to crucially depend on a persistent biochemical mechanism involving an aPKC, PKM ζ (*Pastalkova et al., 2006; Shema et al., 2007; Wang et al., 2016; Gao et al., 2018; Tsokas et al., 2024*). However, both long-term phenomena are observed when PKM ζ is genetically deleted (*Lee et al., 2013; Volk et al., 2013; Tsokas et al., 2016; Tsokas et al., 2024*). These results either

confirm the structural model or point to the existence of a compensatory biochemical mechanism for memory (*Tsokas et al., 2016*) .

Here we found that a second biochemical mechanism for memory comes into play to compensate for the loss of the first. The PKC isoform most closely related to PKMζ, PKCι, which normally plays only a transient role in LTP and short-term memory, becomes persistently active in LTP and long-term memory when PKMζ is genetically ablated (Figures 1, 2). When we eliminate the two persistent biochemical processes by double-knockout there is no enduring hippocampal LTP or long-term memory (Figures 3, 4). These results establish a biochemical mechanism as the leading candidate for how a memory endures, and identifies both PKMζ and PKCι as persistent kinases crucial for sustaining memory, beyond the contribution of any static structural processes necessary for synaptic integrity.

The ι/ζ-dKO exhibits an early transient LTP that could not be sustained into late-phase persistent LTP (Figure 3). In addition, bilateral hippocampal ι/ζ-dKO eliminated long-term spatial memory but did not prevent learning, short-term memory, or expression of the place avoidance behavior (Figure 4). In WT mice, PKCι is a key contributor to early-LTP and short-term memory (*Ren et al., 2013; Wang et al., 2016*); therefore, there must be additional compensation for short-term processes present in the aPKC-dKO.

Our finding that PKCι compensates for the absence of PKMζ raises the question, how is it induced. Compensatory gene expression can be induced after gene knockout by the fragments of mRNA that are produced by transcription upstream of the site of Cre-recombination (*El-Brolosy and Stainier, 2017; El-Brolosy et al., 2019; Ma et al., 2019*). This could explain why PKMζ-KOs produce compensation, but PKMζ-shRNA or PKMζ-antisense oligodeoxynucleotides that retain full-length PKMζ mRNA transcription do not (*Tsokas et al., 2016; Wang et al., 2016*). In medial prefrontal cortex, both early- and late-LTP are absent in PKMζ-KO mice (*Kniffin et al., 2025*). This suggests that the PKCι activation mediating early-LTP in the WT hippocampus may not be available as a biochemical process to compensate for loss of PKMζ in the ζ-KO medial prefrontal cortex (*Sacktor, 2025*).

Once increased, how does PKCι accomplish maintenance? PKMζ maintenance is linked to the kinase's second messenger-independent, persistent activity (*Sacktor et al., 1993*). PKMζ is autonomously active because the kinase is an independent catalytic domain that lacks the PKCζ autoinhibitory regulatory domain (*Sacktor et al., 1993; Hernandez et al., 2003*). PKCι, however, is a full-length PKC isoform with a regulatory domain that inhibits its catalytic domain. Therefore, for PKCι to compensate for PKMζ the aPKC likely requires additional posttranslational mechanisms to persistently activate and localize the kinase at active synapses (Figure 1C). Unlike other isoforms, PKCι can be activated by its regulatory domain binding to postsynaptic proteins such as p62 (*Jiang et al., 2009; Ren et al., 2013*). This activation of PKCι by protein-protein interaction may sustain its kinase activity longer than the transient lipid second messengers that activate the conventional/novel PKCs, allowing one persistent biochemical mechanism to replace the other.

The maintenance properties of PKMζ not only depend on continuous activity but also on continuous binding to the postsynaptic scaffolding protein KIBRA/WWC1 (kidney and brain protein/WW and C2 domain protein 1) (*Tsokas et al., 2024*). This interaction localizes PKMζ to active synapses in a process called persistent synaptic tagging (*Tsokas et al., 2024; Shouval et*

al., 2025). KIBRA also weakly binds PKCι (*Tsokas et al., 2024*). In WT mice, the stronger binding of PKMζ to KIBRA might allow it to replace PKCι at active synapses in the transition from early- to late-LTP. In the hippocampus of PKMζ-KO mice, PKCι at active synapses would not be replaced. PKMζ and PKCι also compete for binding to PAR3 (partitioning defective protein 3), another postsynaptic protein that localizes aPKCs within neurons (*Parker et al., 2013; Zhang and Wei, 2022*). Thus, when PKMζ is genetically deleted, synaptic tags such as KIBRA and PAR3 that are components of the persistent PKMζ mechanism may now shift to PKCι to maintain hippocampus-dependent LTP and long-term memory.

Acknowledgements: P.T. is an Alexander S. Onassis Public Benefit Foundation Scholar.

Funding:

National Institutes of Health grant R37 MH057068 (TCS)

National Institutes of Health grant R01 MH115304 (TCS and AAF)

National Institutes of Health grant R01 NS105472 (AAF)

National Institutes of Health grant R01 MH132204 (AAF)

National Institutes of Health grant R01 NS108190 (PJB and TCS)

The Garry & Sarah S. Sklar Fund (PT)

Author contributions:

Conceptualization: TCS, AAF

Methodology: PT, CH, AG-P, LK, SG

Investigation: PT, CH, AG-P, LK, LMR-V, DAC, KDA, HJHS, SK, BJW, SS, REF-O

Visualization: CH, AG-P

Funding acquisition: TCS, AAF, JEC

Project administration: TCS, AAF

Supervision: TCS, AAF

Writing – original draft: TCS, AAF, PJB, JR

Writing – review & editing: TCS, AAF, PJB, JR, JEC

Competing Interests: The authors declare that they have no competing interests.

Data Availability: All data are available in the main text or the supplementary materials.

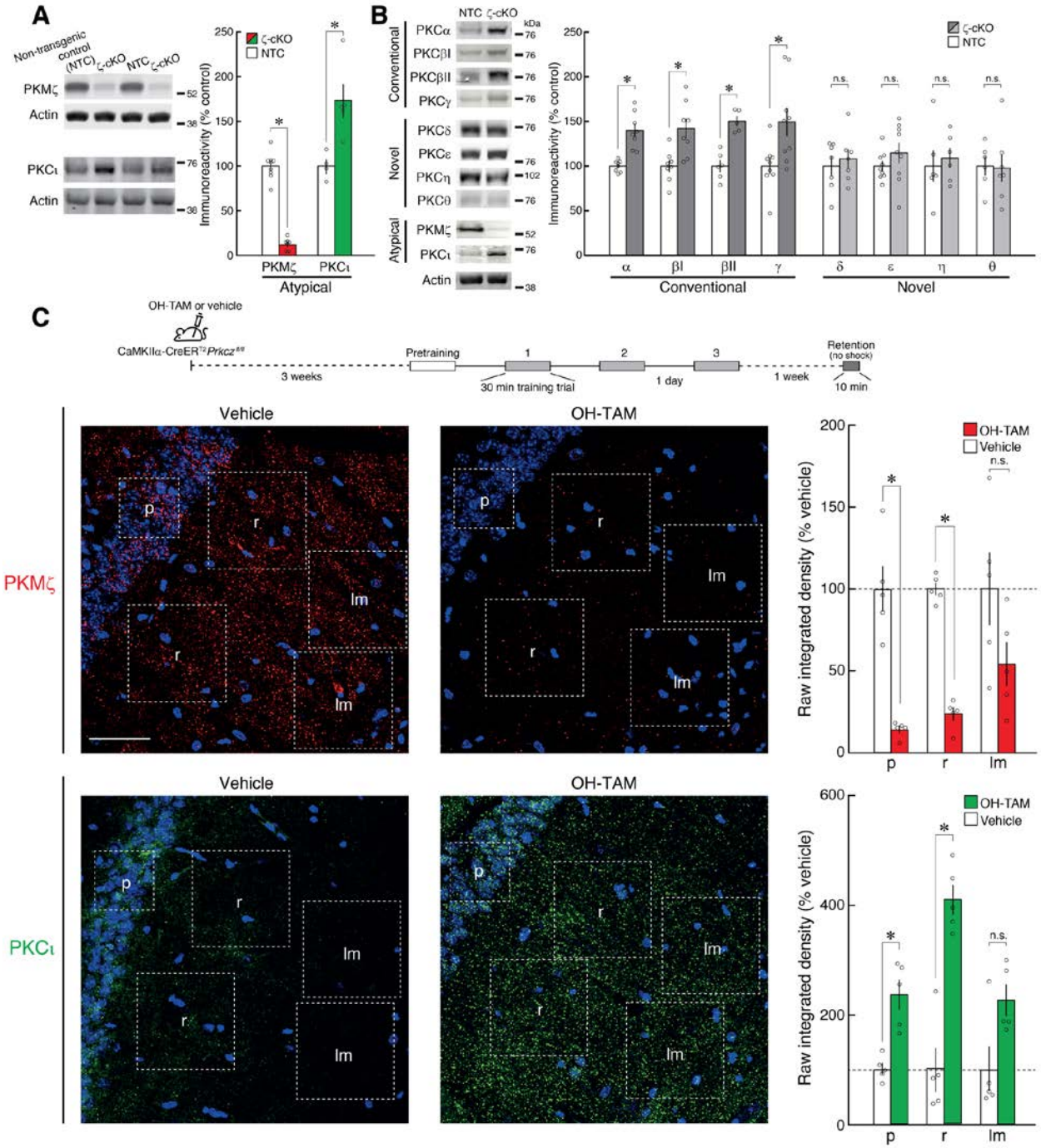

Figure 1. Compensatory increases of atypical PKC ι and conventional, but not novel PKCs, in conditional PKM ζ-KO mouse hippocampus. (**A, B**) Immunoblots of hippocampal extracts from *Camk2a-CreER^{T2}Prkcz$^{fl/fl}$* mice receiving tamoxifen (2 mg/200 µl i.p., 5 daily doses) to activate Cre recombinase selectively in excitatory neurons. Mice are sacrificed 7 days after the last dose. Left, representative immunoblots with Mr markers. Right, mean ± SEM. Significance by two sample Student *t* tests with Bonferroni correction denoted by *; not significant, n.s.; statistics in Figure 1 — table supplement 1A,B. Tamoxifen is a partial PKC antagonist and may still be present after a week (*O'Brian et al., 1985*); therefore, WT mice that also received tamoxifen are non-transgenic controls (NTC). (**A**) PKM ζ decreases and PKC ι

increases in PKMζ-cKO mice. (**B**) Conventional PKCs increase and novel PKCs do not change. For clarity, the actin shown is for PKCs α, ι, and PKMζ immunoblots. (**C**) Immunohistochemistry shows ζ-cKO reduces PKMζ and increases PKCι in CA1 *st. pyramidale* (p) and *radiatum* (r), but not *lacunosum-moleculare* (lm) 1 week after training. Inset above, schematic of experimental protocol. PKMζ is deleted using *Camk2a-CreER*^{T2}*Prkcz*$^{fl/fl}$ mice. Cre is activated using 4-OH tamoxifen (OH-TAM, 2 mg/200 µl i.p., 3 doses every other day). Control mice receive vehicle injections. Active place avoidance training begins 3 weeks later, and 1 week after training memory retention is tested in the absence of shock. Left above, immunohistochemistry reveals reduced PKMζ expression in cell bodies and dendritic compartments of the PKMζ-cKO. Left below, PKCι increases in cell bodies as well as in dendritic compartments where it is ordinarily expressed at low levels. Right, mean ± SEM. Student *t* tests with Bonferroni corrections compared differences in PKMζ and PKCι expression separately in *strata* of CA1 (Figure 1 — table supplement 1C). DAPI staining of nuclei shown in blue. Bar = 50 µm.

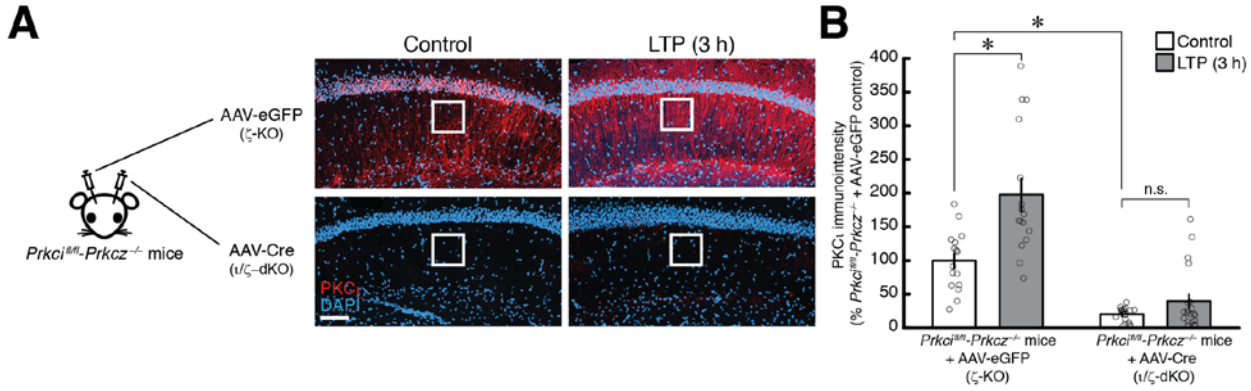

Figure 2. Compensatory increases of PKC ι during hippocampal late-LTP maintenance in *Prkci*$^{fl/fl}$-*Prkcz*$^{-/-}$ mice. (**A**) Left, schematic of experimental protocol shows AAV expressing Cre by CMV promoter injected into ipsilateral hippocampus of a *Prkci*$^{fl/fl}$-*Prkcz*$^{-/-}$ mouse, and control AAV expressing eGFP in contralateral hippocampus. Hippocampal slices are prepared 3 weeks later. Right, representative images of PKC ι-immunohistochemistry from adjacent slices in AAV-eGFP-injected (ζ-KO) hippocampus show PKC ι persistently increases 3 h post-tetanization (top row), and low, unchanging levels of PKC ι in the AAV-Cre-injected (ι/ζ-dKO) hippocampus (bottom row). White boxes show *st. radiatum* regions of interest. (**B**) Mean ± SEM. The two-way ANOVA reveals the main effects of treatment (AAV-Cre [ι/ζ-dKO] vs. AAV-eGFP [ζ-KO], $F_{1,68} = 83.58$, $P < 0.00001$, $\eta^2_p = 0.55$), and stimulation (HFS vs. test, $F_{1,68} = 20.47$, $P = 0.00003$, $\eta^2_p = 0.23$), and an interaction of treatment x stimulation ($F_{1,68} = 9.09$, $P = 0.004$, $\eta^2_p = 0.12$). *Post-hoc* analysis confirms that, compared to the ζ-KO control group, the intensity of PKC ι immunoreactivity was significantly decreased in ι/ζ-dKO (P's < 0.002 for both control and LTP in ι/ζ-dKO), and increased in ζ-KO after HFS ($P = 0.00011$, ζ-KO, n's = 16, ι/ζ-dKO, n's = 20). Intensity of PKC ι immunoreactivity did not change in the ι/ζ-dKO between the control and HFS groups ($P = 0.3$). Bar = 100 µm.

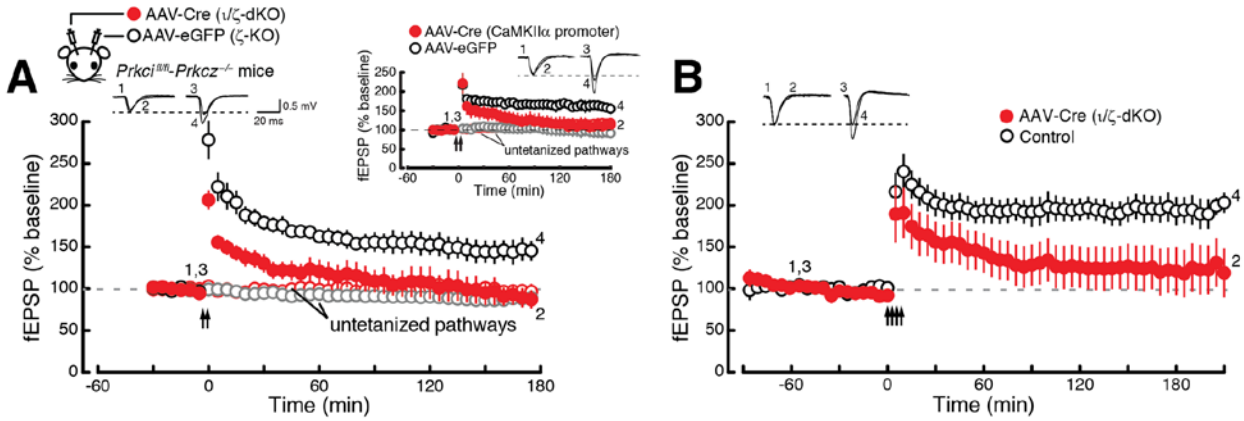

Figure 3. ι/ζ-dKO hippocampus shows transient LTP, but not persistent LTP. (**A**) Late-LTP is absent in ι/ζ-dKO hippocampus. Above left inset, schematic of intrahippocampal injections of AAC-Cre and AAV-eGFP. Middle inset, representative fEPSPs correspond to numbered times in time-course below. Below, filled red circles, AAC-Cre expressed by CMV promoter and HFS with 2 tetanic trains; open red circles, test stimulation of a second synaptic pathway within the hippocampal slice. HFS tetani shown at arrows. Open black circles, AAV expressing eGFP with HFS; open grey circles, with test stimulation. Three-way mixed-design ANOVA reveals main effects of treatment (hippocampal injections of AAV-Cre [ι/ζ-dKO] vs. AAV-eGFP [ζ-KO], $F_{1,20} = 8.45$, $P = 0.0009$, $\eta^2_p = 0.30$), and stimulation (HFS vs. test stimulation, $F_{1,20} = 5.90$, $P = 0.025$, $\eta^2_p = 0.23$), as well as a 3-way interaction among treatment x stimulation x time (5-min average of pre-HFS and 3-h post-HFS, $F_{1,20} = 12.68$, $P = 0.002$, $\eta^2_p = 0.39$). *Post-hoc* analysis confirms established LTP is not maintained in ι/ζ-dKO 3 h after HFS when compared to pre-HFS basal responses ($P = 0.7$). *Post-hoc* analysis also confirms the control hippocampus maintains established LTP ($P = 0.0002$). Test stimulation was unaffected by AAV-Cre or AAV-eGFP injections ($P = 0.9$ and $P = 0.7$, respectively, n's = 6). Right inset, ι/ζ-dKO by CaMKIIα promoter expression of Cre recombinase eliminates late-LTP. Three-way mixed-designed ANOVA reveals interaction between treatment (ζ-KO vs. ι/ζ-dKO) and stimulation (HFS vs. test stimulation, $F_{1,14} = 6.62$, $P = 0.02$, $\eta^2_p = 0.32$), and a 3-way interaction among treatment, stimulation, and time (5 min pre-HFS and 3 h post-HFS, $F_{1,14} = 8.56$, $P = 0.01$, $\eta^2_p = 0.38$). *Post-hoc* analysis confirms that compared to pre-HFS basal responses, LTP is not maintained in ι/ζ-dKO hippocampus 3 h post-HFS ($P = 0.8$) and is maintained in the control hippocampus ($P = 0.003$). Test stimulation was unaffected by AAV-Cre or AAV-eGFP injections ($P = 0.4$ and $P = 0.9$, respectively). ι/ζ-dKO HFS, n = 5; ι/ζ-dKO test, n = 4, ζ-KO HFS, n = 5, ζ-KO test, n = 4. (**B**) LTP does not persist in ι/ζ-dKO mice after the stronger tetanization. ANOVA with repeated measurements reveals main effects of time (5 min pre-HFS, 20 min post-HFS, and 3 h post-HFS, $F_{2,14} = 20.51$, $P < 0.0001$, $\eta^2_p = 0.75$). *Post-hoc* analysis confirms that early-LTP is established in both ι/ζ-dKO and control groups (5 min pre-HFS vs. 20 min post-HFS, $P = 0.005$ and 0.002, respectively), and no difference between these two groups at 20 min post-HFS ($P = 0.6$). However, LTP in ι/ζ-dKO did not persist 3 h (5 min pre-HFS vs. 3 h post-HFS, $P = 0.4$), whereas LTP is intact in control. ($P = 0.008$). The ι/ζ-dKO, n = 5; control, n = 4.

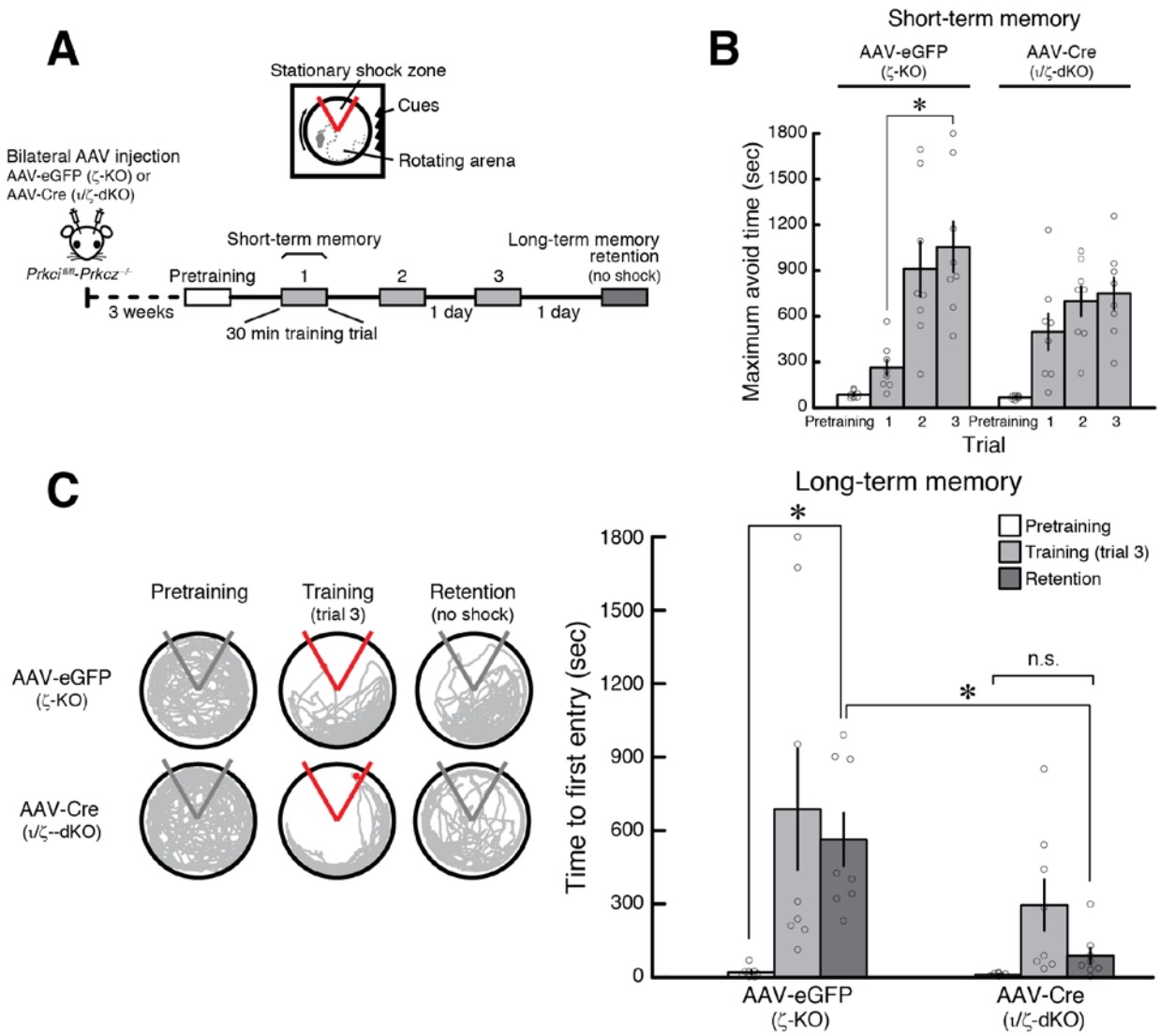

Figure 4. Impaired spatial long-term memory and intact spatial short-term memory in mice with bilateral hippocampal ι/ζ-dKO. (**A**) Above, schematic of active place avoidance training apparatus shows a slowly rotating arena containing a nonrotating shock zone sector (delineated in red). Visual cues located on the walls of the room are needed to avoid the shock zone. Below, protocol for active place avoidance. *Prkci*$^{fl/fl}$-*Prkcz*$^{-/-}$ mice are injected bilaterally in hippocampus with AAV-Cre (ι/ζ-dKO) or AAV-eGFP (ζ-KO, control). (**B**) ι/ζ-dKO does not affect short-term memory as assessed by maximum avoidance time during the first training trial. The contrast analysis reveals that the increases of maximum avoidance time from pretraining to trial 1 are not different between AAV-eGFP-injected and AAV-Cre-injected groups (t_{14} = 1.91, P = 0.08, d = 1.91), indicating both groups of mice successfully established short-term memory. However, the improvement of maximum avoidance time from trial 1 to trial 3 are different between the groups (t_{14} = 2.93, P = 0.01, d = 2.88), suggesting the two groups performed differently between daily training sessions. In addition, the ANOVA with repeated measurement discovers no group effect (AAV-eGFP-injected vs. AAV-Cre-injected, $F_{1,14}$ = 0.56, P = 0.47, η^2_p = 0.04), but significant effects of trial ($F_{3,42}$ = 30.37, P < 0.0001, η^2_p = 0.68), and

interaction ($F_{3,42}$ = 2.93, P = 0.04, η^2_p = 0.17). *Post-hoc* tests confirm that the maximum avoidance time in trial 1 is not different between the two groups (P = 0.14). The AAV-eGFP-injected group improved their performance between trial 1 and trial 3 (P = 0.0002), whereas the AAV-Cre showed no improvement (P = 0.2; n's = 8). These data indicate no differences in short-term memory between AAV-eGFP- and AAV-Cre-injected groups, but only the AAV-Cre-injected group failed to improve between daily trials, suggesting inability to retain avoidance memory across days. (**C**) PKC ι gene ablation impairs long-term memory in *Prkci*$^{fl/fl}$-*Prkcz*$^{-/-}$ mice. Left, representative paths during 10-min of pretraining, at end of training trial 3, and 1-day memory retention. Right, mean ± SEM. The ANOVA with repeated measurement finds main effects of group (AAV-eGFP vs. AAV-Cre, $F_{1,14}$ = 10.53, P = 0.006, η^2_p = 0.43) and training phase (pretraining, trial 3 of training, retention, $F_{2,28}$ = 7.65, P = 0.002, η^2_p = 0.35). *Post-hoc* analysis reveals that the mice with AAV-Cre-injected ι/ζ-dKO hippocampus perform poorer during the memory retention test, compared to AAV-eGFP-injected littermates (P = 0.02). The mice with ι/ζ-dKO hippocampus show no difference between the memory retention test and pretraining trial (P = 0.9), whereas the AAV-eGFP-injected mice show long-term memory is maintained (P = 0.02; n's = 8). In addition, pretraining vs. training trial 3 was significantly different in ζ-KO (P = 0.006), but not in ι/ζ-dKO (P = 0.4).

References

Anderson WW, Collingridge GL. 2007. Capabilities of the WinLTP data acquisition program extending beyond basic LTP experimental functions. *J Neurosci Methods* **162**: 346-356. S0165-0270(07)00002-7 [pii] 10.1016/j.jneumeth.2006.12.018.

Bailey CH, Kandel ER. 1993. Structural changes accompanying memory storage. *Annu Rev Physiol* **55**: 397-426. 10.1146/annurev.ph.55.030193.002145.

Bayer KU, Giese KP. 2024. A revised view of the role of CaMKII in learning and memory. *Nat Neurosci*. 10.1038/s41593-024-01809-x.

Conant GC, Wagner A. 2004. Duplicate genes and robustness to transient gene knock-downs in Caenorhabditis elegans. *Proc Biol Sci* **271**: 89-96. 10.1098/rspb.2003.2560.

Crick F. 1984. Memory and molecular turnover. *Nature* **312**: 101. 10.1038/312101a0.

El Allam A, Alberto EJ, Mercau ME, Dimitrius T, Pramio DT, Krishna M, Bhat KM, Philbrick WM, Schechtman D, Rothlin CV et al. 2024. Functional roles of neural aPKCs in mouse brain development and survival. *bioRxiv:20240522595312*. doi:10.1101/2024.05.22.595312.

El-Brolosy MA, Kontarakis Z, Rossi A, Kuenne C, Gunther S, Fukuda N, Kikhi K, Boezio GLM, Takacs CM, Lai SL et al. 2019. Genetic compensation triggered by mutant mRNA degradation. *Nature* **568**: 193-197. 10.1038/s41586-019-1064-z.

El-Brolosy MA, Stainier DYR. 2017. Genetic compensation: A phenomenon in search of mechanisms. *PLoS Genet* **13**: e1006780. 10.1371/journal.pgen.1006780.

Gao PP, Goodman JH, Sacktor TC, Francis JT. 2018. Persistent increases of PKMζ in sensorimotor cortex maintain procedural long-term memory storage. *iScience* **5**: 90-98.

Gu Z, Steinmetz LM, Gu X, Scharfe C, Davis RW, Li WH. 2003. Role of duplicate genes in genetic robustness against null mutations. *Nature* **421**: 63-66. 10.1038/nature01198.

Han J, Grau-Perales A, Harris RM, Kao H-Y, Pal A, Alarcon JM, Sacktor TC, Martiniani S, Hofmann HA, Fenton AA. 2025. Persistently increased expression of PKMzeta and unbiased gene expression profiles identify hippocampal molecular traces of a long-term active place avoidance memory and 'shadow' proteins. *bioRxiv:101101/20250428651143*.

Hebb DO. 1949. The Organization of Behavior. A Neuropsychological Theory. *New York John Wiley and Sons, Inc London*.

Hernandez AI, Blace N, Crary JF, Serrano PA, Leitges M, Libien JM, Weinstein G, Tcherapanov A, Sacktor TC. 2003. Protein kinase Mζ synthesis from a brain mRNA encoding an independent protein kinase Cζ catalytic domain. Implications for the molecular mechanism of memory. *J Biol Chem* **278**: 40305-40316. 10.1074/jbc.M307065200.

Hsieh C, Tsokas P, Grau-Perales A, Lesburgueres E, Bukai J, Khanna K, Chorny J, Chung A, Jou C, Burghardt NS et al. 2021. Persistent increases of PKMzeta in memory-activated neurons trace LTP maintenance during spatial long-term memory storage. *Eur J Neurosci* **54**: 6795-6814. 10.1111/ejn.15137.

Jiang J, Parameshwaran K, Seibenhener ML, Kang MG, Suppiramaniam V, Huganir RL, Diaz-Meco MT, Wooten MW. 2009. AMPA receptor trafficking and synaptic plasticity require SQSTM1/p62. *Hippocampus* **19**: 392-406. 10.1002/hipo.20528.

Kniffin AR, English EA, Briand LA. 2025. PKMzeta is necessary for long-term depression and long-term potentiation in the medial prefrontal cortex. *The Journal of physiology*. 10.1113/JP289373.

LeBlancq MJ, McKinney TL, Dickson CT. 2016. ZIP It: Neural Silencing Is an Additional Effect of the PKM-Zeta Inhibitor Zeta-Inhibitory Peptide. *J Neurosci* **36**: 6193-6198. 10.1523/JNEUROSCI.4563-14.2016.

Lee AM, Kanter BR, Wang D, Lim JP, Zou ME, Qiu C, McMahon T, Dadgar J, Fischbach-Weiss SC, Messing RO. 2013. Prkcz null mice show normal learning and memory. *Nature* **493**: 416-419. 10.1038/nature11803.

Lisman JE. 1985. A mechanism for memory storage insensitive to molecular turnover: a bistable autophosphorylating kinase. *Proc Natl Acad Sci U S A* **82**: 3055-3057. 10.1073/pnas.82.9.3055.

Ma Z, Zhu P, Shi H, Guo L, Zhang Q, Chen Y, Chen S, Zhang Z, Peng J, Chen J. 2019. PTC-bearing mRNA elicits a genetic compensation response via Upf3a and COMPASS components. *Nature* **568**: 259-263. 10.1038/s41586-019-1057-y.

Madronal N, Gruart A, Sacktor TC, Delgado-Garcia JM. 2010. PKMζ inhibition reverses learning-induced increases in hippocampal synaptic strength and memory during trace eyeblink conditioning. *PloS one* **5**: e10400. 10.1371/journal.pone.0010400.

Matus A. 2000. Actin-based plasticity in dendritic spines. *Science* **290**: 754-758.

Mercau ME, Hackbarth R-M, Liu X, Wang H, Zhang L, Basu MK, Rothlin CV, Ghosh S. 2024. Time-resolved function of cell polarity kinases PRKCZ and PRKCI in CNS myelination. *bioRxiv:20240422589759*.

Miller SG, Kennedy M. 1986. Regulation of brain type II Ca2+/calmodulin-dependent protein kinase by autophosphorylation: a Ca2+-triggered molecular switch. *Cell* **44**: 861-870.

O'Brian CA, Liskamp RM, Solomon DH, Weinstein IB. 1985. Inhibition of protein kinase C by tamoxifen. *Cancer research* **45**: 2462-2465.

Parker SS, Mandell EK, Hapak SM, Maskaykina IY, Kusne Y, Kim JY, Moy JK, St John PA, Wilson JM, Gothard KM et al. 2013. Competing molecular interactions of aPKC isoforms regulate neuronal polarity. *Proc Natl Acad Sci U S A* **110**: 14450-14455. 10.1073/pnas.1301588110.

Pastalkova E, Serrano P, Pinkhasova D, Wallace E, Fenton AA, Sacktor TC. 2006. Storage of spatial information by the maintenance mechanism of LTP. *Science* **313**: 1141-1144. 10.1126/science.1128657.

Ramón y Cajal S. 1894. La fine structure des centres nerveux. 55, 444–468 (1894). *Proc R Soc Lond* **55**: 444-468.

Ren SQ, Yan JZ, Zhang XY, Bu YF, Pan WW, Yao W, Tian T, Lu W. 2013. PKClambda is critical in AMPA receptor phosphorylation and synaptic incorporation during LTP. *The EMBO journal* **32**: 1365-1380. 10.1038/emboj.2013.60.

Sacktor TC. 2025. PKMzeta-knockout mice lack neocortical long-term potentiation: limits of hippocampal compensation and differential memory rescue. *The Journal of physiology*. 10.1113/JP290246.

Sacktor TC, Fenton AA. 2018. What does LTP tell us about the roles of CaMKII and PKMzeta in memory? *Molecular brain* **11**: 77. 10.1186/s13041-018-0420-5.

Sacktor TC, Osten P, Valsamis H, Jiang X, Naik MU, Sublette E. 1993. Persistent activation of the zeta isoform of protein kinase C in the maintenance of long-term potentiation. *ProcNatlAcadSciUSA* **90**: 8342-8346.

Sadeh N, Verbitsky S, Dudai Y, Segal M. 2015. Zeta Inhibitory Peptide, a Candidate Inhibitor of Protein Kinase Mzeta, Is Excitotoxic to Cultured Hippocampal Neurons. *J Neurosci* **35**: 12404-12411. 10.1523/JNEUROSCI.0976-15.2015.

Scharf MT, Woo NH, Lattal KM, Young JZ, Nguyen PV, Abel T. 2002. Protein synthesis is required for the enhancement of long-term potentiation and long-term memory by spaced training. *J Neurophysiol* **87**: 2770-2777.

Schwartz JH. 1993. Cognitive kinases. *Proc Natl Acad Sci U S A* **90**: 8310-8313.

Scott J, Thakar S, Mao Y, Qin H, Hejran H, Lee SY, Yu T, Klezovitch O, Cheng H, Mu Y et al. 2019. Apical-Basal Polarity Signaling Components, Lgl1 and aPKCs, Control Glutamatergic Synapse Number and Function. *iScience* **20**: 25-41. 10.1016/j.isci.2019.09.005.

Seidl S, Braun U, Roos N, Li S, Ludtke TH, Kispert A, Leitges M. 2013. Phenotypical analysis of atypical PKCs in vivo function display a compensatory system at mouse embryonic day 7.5. *PloS one* **8**: e62756. 10.1371/journal.pone.0062756.

Serrano P, Friedman EL, Kenney J, Taubenfeld SM, Zimmerman JM, Hanna J, Alberini C, Kelley AE, Maren S, Rudy JW et al. 2008. PKMζ maintains spatial, instrumental, and classically conditioned long-term memories. *PLoS Biol* **6**: 2698-2706. 08-PLBI-RA-2746 [pii] 10.1371/journal.pbio.0060318.

Serrano P, Yao Y, Sacktor TC. 2005. Persistent phosphorylation by protein kinase Mζ maintains late-phase long-term potentiation. *J Neurosci* **25**: 1979-1984. 10.1523/JNEUROSCI.5132-04.2005.

Shema R, Haramati S, Ron S, Hazvi S, Chen A, Sacktor TC, Dudai Y. 2011. Enhancement of consolidated long-term memory by overexpression of protein kinase Mzeta in the neocortex. *Science* **331**: 1207-1210. 331/6021/1207 [pii] 10.1126/science.1200215.

Shema R, Sacktor TC, Dudai Y. 2007. Rapid erasure of long-term memory associations in the cortex by an inhibitor of PKMzeta. *Science* **317**: 951-953. 317/5840/951 [pii] 10.1126/science.1144334.

Sheng T, Wang S, Qian D, Gao J, Ohno S, Lu W. 2017. Learning-Induced Suboptimal Compensation for PKCiota/lambda Function in Mutant Mice. *Cerebral cortex* **27**: 3284-3293. 10.1093/cercor/bhx077.

Shouval HZ, Hsieh C, Flores-Obando RE, Cano DA, Tracy TE, Sacktor TC. 2025. Maintenance of memory by negative feedback of synaptic protein elimination: modeling KIBRA-PKMzeta dynamics in LTP. *Learning & memory* **32**. 10.1101/lm.054077.124.

Stokes EG, Vasquez JJ, Azouz G, Nguyen M, Tierno A, Zhuang Y, Galinato VM, Hui M, Toledano M, Tyler I et al. 2025. Cationic peptides cause memory loss through endophilin-mediated endocytosis. *Nature*. 10.1038/s41586-024-08413-w.

Tsien RY. 2013. Very long-term memories may be stored in the pattern of holes in the perineuronal net. *Proc Natl Acad Sci U S A* **110**: 12456-12461. 10.1073/pnas.1310158110.

Tsokas P, Grace EA, Chan P, Ma T, Sealfon SC, Iyengar R, Landau EM, Blitzer RD. 2005. Local protein synthesis mediates a rapid increase in dendritic elongation factor 1A after induction of late long-term potentiation. *J Neurosci* **25**: 5833-5843. 10.1523/JNEUROSCI.0599-05.2005.

Tsokas P, Hsieh C, Flores-Obando RE, Bernabo M, Tcherepanov A, Hernandez AI, Thomas C, Bergold PJ, Cottrell JE, Kremerskothen J et al. 2024. KIBRA anchoring the action of PKMzeta maintains the persistence of memory. *Sci Adv* **10**: eadl0030. 10.1126/sciadv.adl0030.

Tsokas P, Hsieh C, Yao Y, Lesburgueres E, Wallace EJ, Tcherepanov A, Jothianandan D, Hartley BR, Pan L, Rivard B et al. 2016. Compensation for PKMzeta in long-term potentiation and spatial long-term memory in mutant mice. *eLife* **5**: e14846. 10.7554/eLife.14846.

Tsokas P, Ma T, Iyengar R, Landau EM, Blitzer RD. 2007. Mitogen-activated protein kinase upregulates the dendritic translation machinery in long-term potentiation by controlling the mammalian target of rapamycin pathway. *J Neurosci* **27**: 5885-5894. 27/22/5885 [pii] 10.1523/JNEUROSCI.4548-06.2007.

Tsokas P, Rivard B, Hsieh C, Cottrell JE, Fenton AA, Sacktor TC. 2019. Antisense Oligodeoxynucleotide Perfusion Blocks Gene Expression of Synaptic Plasticity-related Proteins without Inducing Compensation in Hippocampal Slices. *Bio Protoc* **9**. 10.21769/BioProtoc.3387.

Tullis JE, Larsen ME, Rumian NL, Freund RK, Boxer EE, Brown CN, Coultrap SJ, Schulman H, Aoto J, Dell'Acqua ML et al. 2023. LTP induction by structural rather than enzymatic functions of CaMKII. *Nature* **621**: 146-153. 10.1038/s41586-023-06465-y.

Volk LJ, Bachman JL, Johnson R, Yu Y, Huganir RL. 2013. PKM-zeta is not required for hippocampal synaptic plasticity, learning and memory. *Nature* **493**: 420-423. 10.1038/nature11802.

Wang S, Sheng T, Ren S, Tian T, Lu W. 2016. Distinct Roles of PKCiota/lambda and PKMzeta in the Initiation and Maintenance of Hippocampal Long-Term Potentiation and Memory. *Cell Rep* **16**: 1954-1961. 10.1016/j.celrep.2016.07.030.

White JK, Gerdin AK, Karp NA, Ryder E, Buljan M, Bussell JN, Salisbury J, Clare S, Ingham NJ, Podrini C et al. 2013. Genome-wide generation and systematic phenotyping of knockout mice reveals new roles for many genes. *Cell* **154**: 452-464. 10.1016/j.cell.2013.06.022.

Zhang L, Wei X. 2022. The Roles of Par3, Par6, and aPKC Polarity Proteins in Normal Neurodevelopment and in Neurodegenerative and Neuropsychiatric Disorders. *J Neurosci* **42**: 4774-4793. 10.1523/JNEUROSCI.0059-22.2022.

Supplementary Materials

Antibodies for immunoblotting	Vendor and catalog number	Concentration
aPKC		
PKMζ (C2)	Sacktor Lab (*Hernandez et al., 2003*)	1:20,000
PKCι (E-7)	Santa Cruz sc-376344	1:200
p-PKC		
p-T410 PKCζ (H2)	Santa Cruz sc-271962	1:200
Phospho-PKC (pan) (ζ Thr410) (190D10)	Cell Signaling Technology #2060	1:100
cPKC		
α (H-7)	Santa Cruz sc-8393	1:200
βI (E-3)	Santa Cruz sc-8049	1:500
βII (F-7)	Santa Cruz sc-13149	1:100
γ (C-4)	Santa Cruz sc-166385	1:200
n-PKC		
δ [EPR17075]	Abcam ab182126	1:100
ε (E-5)	Santa Cruz sc-1681	1:1000
η [EPR18513]	Abcam ab179524	1:200
θ (E-7)	Santa Cruz sc-1680	1:100
Other		
CaMKIIα	ThermoFisher (Invitrogen) 137300	1:100
p-CaMKII [T286]	Cell Signaling Technology #3361	1:100
Actin	Sigma A4700	1:5000

Key resources table.

Materials and Methods:

Reagents: Unless otherwise stated, reagents were from MilliporeSigma.

Animals: Male mice were on C57BL/6 background and at least 4-months-old for all experiments. The PKMζ-null mouse line was previously described (*Lee et al., 2013*) and provided by Robert O. Messing (Univ. Texas at Austin, TX, USA). Conditional PKMζ and PKCι mice were generated by Sourav Ghosh as previously described (*Scott et al., 2019; El Allam et al., 2024; Mercau et al., 2024*). *Camk2a-CreER*^{T2} mice were from Jackson Labs. Tamoxifen vehicle for i.p. injections was sunflower seed oil.

Hippocampal slice recording and stimulation: Acute mouse hippocampal slices (450 µm) were prepared as previously described (*Tsokas et al., 2016; Tsokas et al., 2019*). Hippocampi were dissected, bathed in ice-cold dissection buffer, and sliced with a McIlwain tissue slicer in a cold room (4˚C). The dissection buffer contained (in mM): 125 NaCl, 2.5 KCl, 1.25 NaH_2PO_4, 26 $NaHCO_3$, 11 glucose, 10 $MgCl_2$, and 0.5 $CaCl_2$, and was bubbled with 95% O_2/5% CO_2 to maintain pH at 7.4. After dissection the slices were transferred to an Oslo-type interface recording chamber (31.5 ± 1°C) (*Tsokas et al., 2019*). The recording superfusate consisted of (in mM): 118 NaCl, 3.5 KCl, 2.5 $CaCl_2$, 1.3 $MgSO_4$, 1.25 NaH_2PO_4, 24 $NaHCO_3$, and 15 glucose, bubbled with 95% O_2/5% CO_2, with a flow rate of 0.5 ml/min.

Field EPSPs were recorded with a glass extracellular recording electrode (2–5 MΩ) placed in the CA1 *st. radiatum*, and concentric bipolar stimulating electrodes (CBBRE75 and 30200; FHC, Bowdoin, ME) were placed on either side within CA3 or CA1. Test stimulation rate was once every 30 sec, alternating every 15 sec between stimulating electrodes. Based upon a pre-established exclusion criterion, a slice was not used if fEPSP spike threshold was <2 mV on initial input-output analysis. Pathway independence was confirmed by the absence of paired-pulse facilitation between the two pathways. A single stimulating electrode was used for immunocytochemistry with a test stimulation rate of once every 30 sec. HFS optimized to produce a relatively rapid onset of protein synthesis-dependent late-LTP, consisted of two 100 Hz-1 s tetanic trains, at 25% of spike threshold, spaced 20 sec apart (*Tsokas et al., 2005*). HFS optimized to produce maximal late-LTP consisted of four 100 Hz-1 s tetanic trains, at 25% of spike threshold, spaced 5 min apart (*Scharf et al., 2002; Serrano et al., 2005*). The maximum slope of the rise of the fEPSP was analyzed on a PC using the WinLTP data acquisition program (*Anderson and Collingridge, 2007*).

Immunoblots and Immunohistochemistry: Immunoblots of total hippocampus were performed as previously described, using antibodies in Key Resources Table (*Tsokas et al., 2016*). Immunoblots were stained with multiple antisera to visualize multiple PKCs on the same immunoblot. To conserve antisera the immunoblots were cut to isolate the relevant proteins based on molecular weight. Isoforms with similar molecular weights were either stained with antisera of different species or on separate blots.

Quantitative immunohistochemistry for Figure 2 and Figure 3 — figure supplement 1 was as described (*Hsieh et al., 2021; Tsokas et al., 2024*), using mouse anti-PKCι primary antibody (1:1000, E-7, Santa Cruz SC-376344).

Immunohistochemistry for Figure 1C was performed as follows. Free-floating sections were permeabilized with phosphate-buffered saline (PBS) containing 0.1% Tween20 (PBS-T) for 1 h at room temperature and blocked with 10% normal goat serum in PBS-T (blocking

buffer) for 2.5 h at room temperature. One batch of sections was incubated overnight at 4 °C with rabbit anti-PKMζ C-2 antisera primary antibody (1:1,000) (*Hernandez et al., 2003*) and a second batch of sections with rabbit anti-PKCι (1:1000, Cell Signaling #2998S) in blocking buffer. After washing 3 times for 10 min each in PBS-T, both batches of sections were incubated with the secondary antibody goat anti-rabbit-Alexa 647 (1:500 in blocking buffer; Jackson ImmunoResearch) for 2 h at room temperature. After washing 3 times for 10 min each in PBS-T and extensive washing with PBS, the sections were mounted with Vectashield with 4′,6-diamidino-2- phenylindole (DAPI, Vector Laboratories). Three sections from each mouse were examined using an upright Leica SP8 confocal microscope and analyzed using ImageJ (version 1.53a). For each section, 8.5 µm-thick Z-stacks of the dorsal CA1 were created using the maximum intensity projection function in ImageJ. For each *st. pyramidale, radiatum*, and *lacunosum-moleculare*, two square regions of interest were centered in each stack. Measurements were made from each mouse in each region of interest. The raw integrated density (defined as the sum of the values for all pixels) of the Z-stack region of interest expressing the fluorescent label was measured for the volume of target pixels, and the average of each measurement was taken as representative for the region and each mouse.

AAV injections: Mice were anesthetized in a closed chamber filled with the inhalation anesthetic isoflurane (RWD Life Science, R510-22-10), and then fixed in a stereotaxic apparatus (Stoelting Co.). Anesthesia was maintained with isoflurane inhalation (1%–2.5% via trachea). The eyes of the mice were safeguarded using erythromycin ophthalmic ointment (0.5%). The skull was exposed and cleaned using 3% hydrogen peroxide. Small holes in the skull were then drilled with the following stereotaxic coordinates: left hippocampus (triple injection: AP: -1/ ML: -0.7/ DV: -1.65; AP: -1.8/ ML: -1.5/ DV: -2; AP: -2.7/ ML: -2/ DV: -2, below the skull surface) and right hippocampus (triple injection: AP: -1/ ML: +0.7/ DV: -1.65; AP: -1.8/ ML: +1.5/ DV -2; AP: -2.7/ ML: +2/ DV: -2, below the skull surface). The virus was injected using a 34-gauge needle with a Hamilton syringe at 0.1 µl/min rate into target regions. At all injected points, the tip of the needle was positioned 0.05 mm below the target coordinate and returned to the target site after 2 min. After injection, the needle stayed in place for an additional 7 min and was slowly withdrawn. AAVs expressing Cre-recombinase and eGFP were from Addgene. For physiology, 0.5 ul of virus pENN.AAV.CMVs.PI.Cre.rBG (AAV2.9) (1 x 10^{13} viral genomes [vg]/ml) was injected into one CA1, and 0.5 ul of virus pAAV.CMV.PI.EGFP.WPRE.bGH (AAV2.9) (1 x 10^{13} vg/ml) was injected in the contralateral side. Virus pENN.AAV.CamKIIa 0.4 Cre SV40 (AAV2.9) (1 x 10^{13} vg/ml) was used to express Cre-recombinase by the CaMKIIα promoter.

Conditioning: All experiments were performed blindly. Active place avoidance was conducted with a commercial computer-controlled system (Bio-Signal Group, Acton, MA). The mouse was placed on a 40-cm diameter circular arena rotating at 1 rpm. The specialized software, Tracker (Bio-Signal Group, Acton, MA), was used to detect the animal's position 30 times per second by video tracking from an overhead camera. A clear wall made from polyethylene terephthalate glycol-modified (PET-G) was placed on the arena to prevent the animal from jumping off the elevated arena surface. A 5-pole shock grid was placed on the rotating arena, and the shock was scrambled across the 5-poles when the mouse entered the shock zone. All experiments used the “Room+Arena-“ task variant that challenges the mouse on the rotating arena to avoid a shock zone that was a stationary 60° sector (*Pastalkova et al., 2006*). Every 33 ms, the software determined the mouse’s position, whether it was in the shock zone, and whether to deliver shock. After the animal enters the shock zone for 500 ms, a constant current foot-shock (60 Hz, 500 ms)

was delivered and repeated with the interval of 1500 ms until the mouse left the shock zone. The shock intensity was 0.2 or 0.3 mA, which was the minimum amplitude to elicit flinch or escape responses. The animal was forced to actively avoid the designated shock zone because the arena rotation periodically transported it into the shock area.

The tracked animal positions with timestamps were analyzed offline (TrackAnalysis, Bio-Signal Group, Acton, MA) to extract several end-point measures. The time to first enter the shock zone estimates ability to avoid shock and was taken as an index of between-session long-term place avoidance memory. The maximum time without receiving a shock within each session estimates the within-session short-term place avoidance memory. A pretraining period on the apparatus equivalent in time to a training session, but without shock, was provided, and the time to first entry and between pretraining entrances into the shock zone with the shock off was recorded.

The training schedule was as follows: 1 day after a 30-min pretraining session, the animals received three 30-min training trials, with an intertrial interval of 1 day. Long-term memory retention was tested the following day without shock. Pre-established exclusion criterion was if cannulae were found to be incorrectly targeted. No mice were excluded.

Statistics: Sample sizes vary for the different experimental approaches (biochemistry, extracellular field potential physiology, and behavior). The hypothesis that PKMζ is compensated predicts all-or-none effects in the experiments, and this provided a basis for sample size estimates. Power analyses were performed using G*Power Version 3.1.9.7 with $\alpha = 0.05$ and $\beta = 0.8$ and large effect sizes of 1.5–2.0. The effect size estimates were based on prior studies that demonstrated essentially all-or-none effects of PKMζ inhibition on the immunoblot, immunohistochemical, physiological, and behavioral assays used here (*Tsokas et al., 2016; Hsieh et al., 2021; Tsokas et al., 2024*). Two-population Student *t* tests with Bonferroni corrections were performed to compare protein levels by immunoblot and immunocytochemistry in the PKMζ-cKO and control mice. For LTP experiments the responses to test stimuli were averaged across 5 min for statistical comparisons. Repeated measures ANOVA was used to compare the change in the potentiated response at the time points described. Multi-factor comparisons were performed using mixed-design ANOVA with repeated measures, as appropriate. The degrees of freedom for the critical *t* values of the *t* tests and the *F* values of the ANOVAs are reported as subscripts. *Post-hoc* multiple comparisons were performed by Newman-Keuls tests as appropriate. Statistical significance was accepted at $P < 0.05$. Effect sizes for binary comparisons and one-way ANOVAs are reported as Cohen's *d* and as η^2_p for multi-factor ANOVA effects.

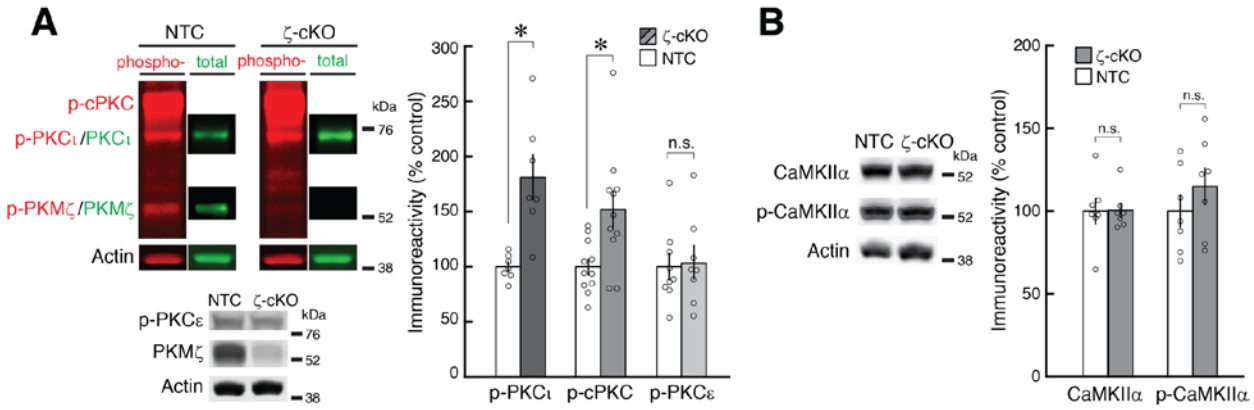

Figure 1 — figure supplement 1. ζ-cKO increases activation-loop-phosphorylation state of atypical PKC ι and conventional PKCs, but not novel PKC ε or CaMKIIα autophosphorylation. (**A**) Left, above, representative immunoblots show increases in activation-loop phosphorylated PKC ι (p-PKC ι) and conventional-PKCs (p-cPKCs) in PKM ζ-cKO mice. Red, phospho-PKCs; green, total PKCs from the same samples. Mr's shown at right. Below, p-PKC ε, recognized by its higher Mr, does not change. Right, mean ± SEM (**B**) Levels of total CaMKIIα and T286-autophosphorylated CaMKIIα do not change in ζ-cKO hippocampus. Statistics in Figure 1 — table supplement 2.

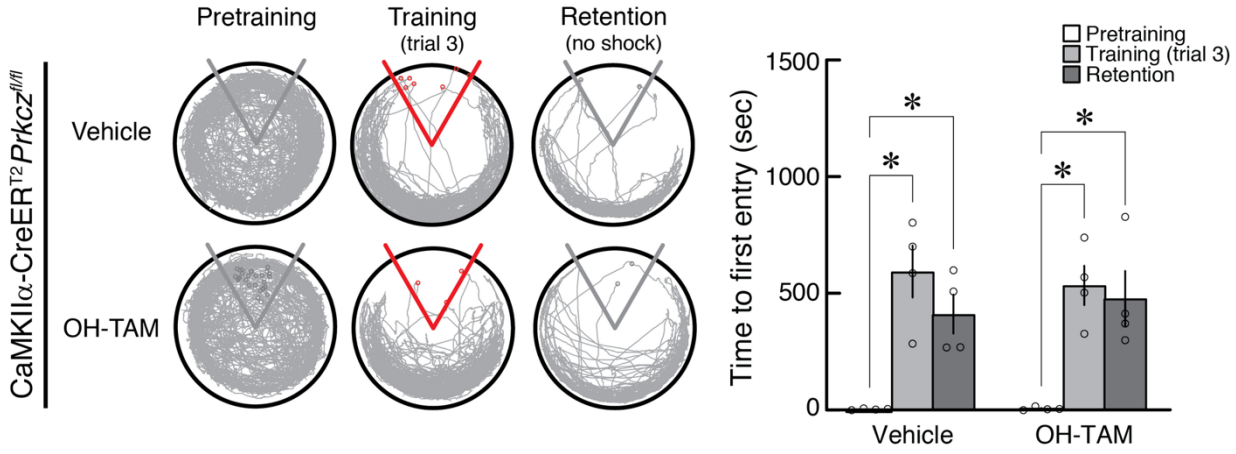

Figure 1 — figure supplement 2. Compensation for spatial memory in ζ-cKO mice. Two-way ANOVA (treatment X training) revealed a significant effect of training ($F_{1.662, 9.972}$ = 41.93, P < 0.0001), but not an effect of treatment ($F_{1, 6}$ < 0.001, P = 1.0) or their interaction ($F_{2, 12}$ = 0.48, P = 0.6). Further comparisons using Bonferroni-corrected tests revealed significant differences between pretraining and training (Trial 3) (P = 0.002) and pretraining and retention (P = 0.001), but no differences between training (Trial 3) and retention (P = 0.1). Moreover, comparison also revealed significant differences between pretraining and training (Trial 3) in both vehicle and 4-OH tamoxifen groups (P = 0.02 and P = 0.01, respectively) and between pretraining and retention in both vehicle and 4-OH tamoxifen groups (P = 0.03 and P = 0.05, respectively), confirming the treatment groups did not behave differently.

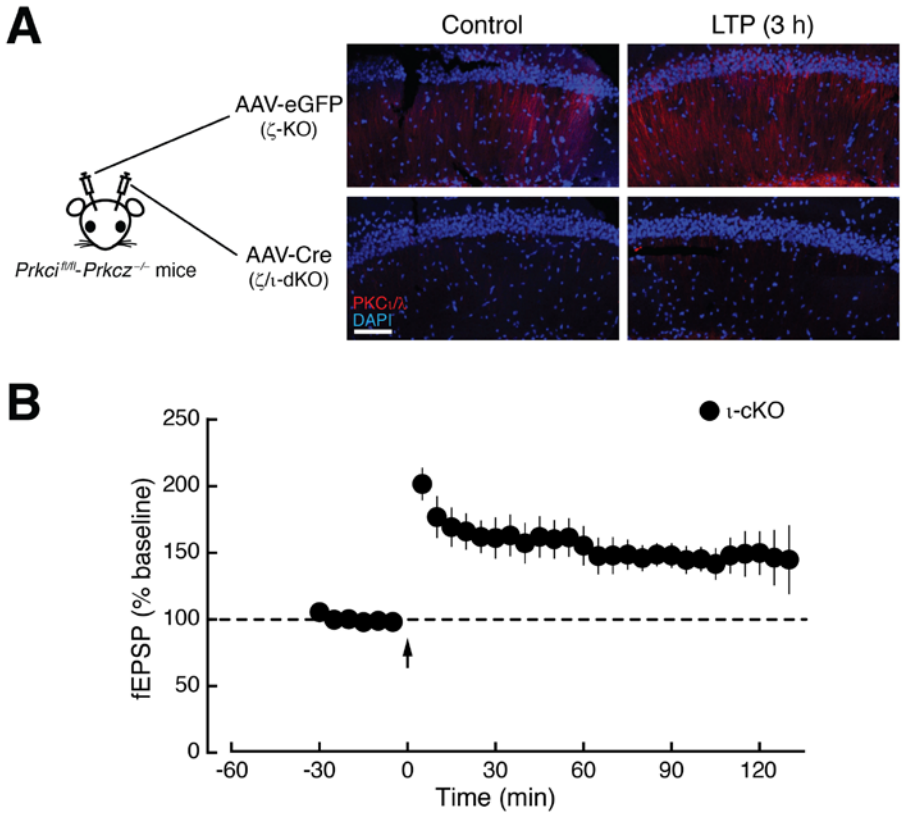

Figure 3 — figure supplement 1. (**A**) **Representative immunohistochemistry of AAV expressing Cre-recombinase by CaMKIIα promoter in *Prkci*$^{fl/fl}$-*Prkcz*$^{-/-}$ mice shows loss of PKC ι in ι/ζ-cKO hippocampus and compensatory increase in PKCι during LTP maintenance in contralateral control eGFP-injected hippocampus.** Left, schematic of sites of injection; right, PKC ι immunohistochemistry. DAPI stains nuclei in CA1. Bar = 100 µm. (**B**) **ι-cKO hippocampus shows compensated LTP.** AAV expressing Cre-recombinase by CaMKIIα promoter was injected into *Prkci*$^{fl/fl}$-*Prkcz*$^{+/+}$ mice. Loss of early-LTP is compensated in the PKC ι-cKO as in previous reports (Sheng et al., 2017). Paired t-test reveals early-LTP is established at 20 min post-tetanization (t_3 = 4.76, P = 0.02, Cohen's d = 3.41, n = 4).

Isozyme / region	Non-transgenic control (NTC)		ζ-cKO		Degree of freedom	*t*	*P*	Cohen's *d*
	Mean ± SEM	n	Mean ± SEM	n				
(A)								
aPKC								
PKMζ	**100 ± 4.9**	**9**	**11.8 ± 2.4**	**8**	**15**	**15.4**	**< 0.0001**	**7.5**
PKCι	**100 ± 7.3**	**4**	**172.4 ± 18.4**	**5**	**7**	**3.9**	**0.01**	**2.2**
(B)								
cPKC								
α	**100 ± 2.3**	**8**	**140.0 ± 7.0**	**8**	**14**	**5.4**	**< 0.0001**	**2.7**
βI	**100 ± 6.2**	**8**	**142.1 ± 10.6**	**8**	**14**	**3.4**	**0.004**	**1.7**
βII	**100 ± 6.3**	**6**	**150.2 ± 5.5**	**5**	**9**	**5.9**	**0.0002**	**3.6**
γ	**100 ± 8.6**	**9**	**149.6 ± 15.4**	**9**	**16**	**2.8**	**0.01**	**1.3**
nPKC								
δ	100 ± 10.4	7	108.2 ± 10.3	7	12	0.6	0.6	0.3
ε	100 ± 5.3	9	114.8 ± 11.0	9	16	1.2	0.2	0.6
η	100 ±17.1	6	109.0 ± 10.9	6	10	0.4	0.7	0.3
θ	100 ± 10.1	6	97.7 ± 14.9	7	11	0.1	0.9	0.1
(C)								
PKMζ								
pyramidale	**100 ± 13.6**	**5**	**14.1 ± 2.1**	**5**	**8**	**6.2**	**0.0003**	**3.9**
radiatum	**100 ± 3.6**	**5**	**23.6 ± 3.9**	**5**	**8**	**14.4**	**<0.0001**	**9.1**
lac-mol	100 ± 22.0	5	54.2 ± 13.2	5	8	1.8	0.1	1.1
PKCι								
pyramidale	**100 ± 9.8**	**5**	**235.3 ± 26.4**	**5**	**8**	**4.8**	**0.001**	**3.0**
radiatum	**100 ± 36.9**	**5**	**411.2 ± 26.2**	**5**	**8**	**6.9**	**0.0001**	**4.3**
lac-mol	100 ± 40.1	5	226.7 ± 26.7	5	8	2.6	0.03	1.7

Figure 1 — table supplement 1. Statistics for data presented in Figure 1. Significant differences with Bonferroni correction are in bold.

Kinase	Mean ± S.E.M.	n	Mean ± S.E.M.	n	Degree of freedom	*t*	*P*	Cohen's *d*
(**A**)								
p-PKC								
p-PKCι	**100 ± 4.0**	**7**	**181.1 ± 19.8**	**7**	**12**	**4.0**	**0.002**	**2.1**
p-cPKC	**100 ± 7.1**	**11**	**151.4 ± 16.4**	**11**	**20**	**3.3**	**0.009**	**1.2**
p-PKCε	100 ± 11.7	9	104.0 ± 14.2	8	15	0.2	0.8	0.1
(**B**)								
CaMKIIα	100 ± 7.63	7	96.33 ± 1.95	6	11	0.43	0.67	0.24
p-CaMKIIα	100 ± 9.65	7	114.94 ± 11.17	7	12	1.01	0.33	0.54

Figure 1 — table supplement 2. Statistics for data presented in Figure 1 — figure supplement 1. Significant differences with Bonferroni correction are in bold.